

Multi-layer Default Risk Contagion in Inter-banking Networks

Xiaoqi Bi¹, Alec Koppel², Carolyn L. Beck¹

¹Industrial & Enterprise Systems Engineering ²JP Morgan AI Research, New York, NY
University of Illinois at Urbana-Champaign, Urbana, IL

{xiaoqib2,beck3}@illinois.edu alec.koppel@jpmchase.com

Abstract—Default risk spreading processes in inter-banking networks are commonly viewed as contagion processes, with inter-bank loans as a direct spreading channel and overlapping investment portfolios as an indirect channel. In this paper, we propose a multi-layer network default risk contagion model to incorporate additional panic contagions in the networks of depositors as a novel augmentation of previous models, allowing for the direct characterization of the “bank run” phenomenon, where many depositors simultaneously issue withdrawal requests. Our model is calibrated with post-COVID pandemic data, accounting for macroeconomic factors such as fluctuating interest rates and asset bubbles. Using system identification methods, we analyze relationships between federal interest rates and market prices, and formulate an optimal control problem to mitigate default risk via liquidity ratio requirements in stress tests. Long-term simulation results are presented to reveal threshold structures under varying contagion parameters.

I. INTRODUCTION

Over the past two decades, there has been substantial interest in exploring the modeling, analysis, and control of financial risk contagion, particularly those approaches that incorporate network topology and structures [1], [2], [3]. Additionally, considerable research has focused on understanding how financial risk propagates, often categorized into counter-party risks and risks associated with holding common assets [4], [5]. Following the occurrence of three consecutive regional bank defaults within two months in the United States during the spring of 2023, specifically, the failures of Silicon Valley Bank (SVB), Signature Bank, and First Republic Bank, financial or default risk contagion has come to the fore again in spread process research. In this work, we focus on improving the representational granularity of modeling the spread of financial risk.

Recent studies have explored systemic risk in inter-banking networks using layered models, examining channels such as common asset holdings, asset correlations, and inter-bank loans, but often neglecting behavioral contagion among financial risk holders [6], [7], [8], [9]. Emerging research has begun incorporating factors such as risk sentiment contagion and social behaviors of credit risk holders. For instance, [10] analyzes the coupling effect between credit risk contagion and sentiment contagion, considering factors like risk attitude and supervision behaviors. [11] proposes a dual-layer model for credit risk contagion among entrepreneurs and their enterprises, incorporating the influence of entrepreneurs’ risk attitudes on credit risk spreading processes. In [12] the

authors examine inter-bank runs triggered by panic, focusing on scenarios where the creditor-bank demands early repayment of inter-bank loans upon learning of a debtor-bank’s insolvency. However, this latter study does not address bank runs initiated by depositors. Authors in [13] investigated the dual contagion of high-frequency volatility tail risk and investor’s sentiment in the stock market.

During the 2023 banking crisis in the United States, both SVB and First Republic Bank filed for bankruptcy following bank runs, where a significant number of depositors simultaneously withdrew funds from their deposit accounts due to concerns about the solvency of the banks. To address this distinctive factor, in this paper, we propose a model incorporating a novel layer of panic contagion over the (social) contact networks of depositors during banking crises, explicitly characterizing “intra-bank runs.” This approach allows a direct connection between sentiment contagion among the depositors to bank asset dynamics, and incorporates varying levels of depositor network connectedness simultaneously, which is crucial for realistically modeling default risk contagion among banks [14]. To our knowledge, this is the first model to connect inter-bank asset dynamics, market price fluctuations, depositor panic, and resulting bank defaults. Using ARMA models and time-series data, we calibrate our model to reflect post-pandemic and 2023 banking crisis characteristics, including interest rate fluctuations, inflation, and market dynamics. We address default risk mitigation through an optimal control formulation with liquidity requirements as the control input, presenting simulation results that reveal threshold structures in long-term contagion dynamics.

II. FINANCIAL RISK CONTAGION MODELS

We propose a multi-layer default risk model that incorporates interactive layers of inter-bank and inter-depositor contagion dynamics. On one hand, risk proliferates through the inter-bank layer, influencing banks’ assets; on the other hand, it spreads through the inter-depositor layer, affecting banks’ liabilities. These two dynamics define the asset-liability imbalance, and hence whether the bank defaults.

A. Inter-bank contagion: asset dynamics of banks

We first define the asset dynamics of banks within the inter-bank network and the associated financial risk contagion. Inspired by [15], we consider an inter-bank network of N banks with a “core-periphery” structure, a common configuration in financial networks [1], [16], [18]. Each bank’s

*This work has been partially funded by NSF grant ECCS 20-32321.

assets are divided into four categories: cash equivalents; long-term bond investments, securities and cryptocurrencies; other non-liquid assets; and inter-bank loans. We denote these four components of assets for bank k at time t as $C^k(t)$, $Q^k(t)$, $O^k(t)$, and $\sum_h x_{kh}(t)$, respectively, where $k, h \in [N]$. Here $x_{kh}(t) = g(y_{kh}(t))$, where $x_{kh}(t), y_{kh}(t)$, respectively, represent the size of inter-bank loans that bank h is able to pay back to, and owes to bank k at time t . The specific form of the function $g(\cdot)$ is discussed in a later section. The total assets of bank k at time t is then given by

$$A^k(t) = C^k(t) + Q^k(t) + O^k(t) + \sum_{h \neq k} x_{kh}(t). \quad (1)$$

Investment $Q^k(t)$ is determined by both the investment portfolio and the prevailing market prices, represented by

$$Q^k(t) := \sum_m Q_{km}(t) P_m(t, \tau(t)). \quad (2)$$

Here $Q_{km}(t)$ denotes the amount of investment of type m held by bank k at time t , and $P_m(t, \tau(t))$ represents the current market price per unit of investment type m . We further assume that these prices are influenced by both time and the current federal interest rate $\tau(t)$. Within this layer, default risk proliferates through inter-bank loans, $x_{kh}(t)$, and overlapping portfolios, $Q^k(t)$.

Note that by making assumptions that the market price of investments fluctuates over time in response to general market conditions (indicated by the federal interest rate, τ), we extend the contagion model initially proposed in [15] from a single-shock scenario to a long-term contagion model, where a series of financial shocks may arise due to market fluctuations. This augmentation enables us to incorporate macroeconomic influences, which are particularly significant in periods like the post-pandemic market era.

B. Inter-depositor contagion: liability dynamics of banks

With the asset dynamics now defined, we focus on the dynamics of bank liability, which consists of the inter-bank loans a bank owes to other banks in the system, denoted as $Y^k(t) := \sum_{h \neq k} y_{hk}(t)$, as well as the deposits owed to the bank's depositors, represented by $V^k(t)$, for all $k \in [N]$. A critical contribution of our model is addressing the "bank-run" phenomenon, which predominantly drives the liability dynamics.

Bank runs, primarily fueled by fear or panic, frequently lead to bank defaults [17], [18]. Considerable effort has been devoted to modeling the propagation of emotions or (mis)information using epidemic models due to their analogous agent-to-agent transmission mechanism; see e.g., [19], [20]. As a longstanding and classic option in the information contagion literature [21], [22], we employ a classic networked *SIR* model to capture sub-layers of rumor contagion involving a bank's insolvency and the subsequent panic reactions from the bank's depositors to these rumors and their corresponding funds withdrawal. Consider the social network for bank k characterized by an adjacency matrix W^k , where

W_{ij}^k represents the strength of communication/influence between depositor i and depositor j . The networked panic contagion model we propose is given by

$$\begin{aligned} \dot{s}_i^k(t) &= -\beta_i s_i^k(t) \sum_j W_{ij}^k p_j^k(t) \\ \dot{p}_i^k(t) &= \beta_i s_i^k(t) \sum_j W_{ij}^k p_j^k(t) - \gamma_i p_i^k(t) \\ \dot{r}_i^k(t) &= \gamma_i p_i^k(t), \end{aligned} \quad (3)$$

where $s_i(t), p_i(t), r_i(t)$, respectively, denote at time t the probability of depositor i being susceptible to panic, in a panicked state, and having resolved a panicked state. For client i , β_i is the transmission rate of the panic, and γ_i is the recovery rate from panic, i.e., the rate at which panic is adequately resolved. Note that the model in (3) is based on the classic mean-field approximation of a continuous-time agent-based *SIR* compartment model, therefore assuming independent evolution processes between agents [23]. We assume that panic may be triggered by the publication of a quarterly banking profile (QBP) when the report shows a significant financial loss or a shortage of capital. We also assume that each depositor i has a panic threshold denoted as $b_i(\tau(t))$. Depositors will withdraw funds if their panic level $p_i(t)$ exceeds this threshold, i.e., if

$$p_i(t) > b_i(\tau). \quad (4)$$

That is, depositors' decisions are influenced by both their panic level and current financial market conditions. For example, in a volatile market, depositors might choose to keep their money in the bank even if their panic level is high. Let $d_i^k(t)$ be the collective value of deposits client i has at bank k at time t . Then, the expected amount of funds withdrawn from bank k during a panic contagion can be computed as

$$V^k(t) = \sum_i d_i^k(t) 1_{\{p_i(t) > b_i(\tau(t))\}}, \quad (5)$$

where $1_{\{p_i(t) > b_i(\tau(t))\}}$ is the indicator function that depositor i has a panic level that exceeds their withdrawal decision threshold $b_i(\tau(t))$. (5) directly connects the assets and liability dynamics of banks, which is made explicit in the following section.

C. Default risk contagion model

By definition, banks default when unable or unwilling to fulfill required interest or repayment on a debt [24]. Therefore, with the previously defined asset and liability dynamics, we can define the default of a bank as

$$D^k(t) = 1_{\{A^k(t) < V^k(t) + Y^k(t)\}}, \quad k = 1, \dots, N. \quad (6)$$

The number of bank defaults at time t can be consequently computed as $D(t) = \sum_{k=1}^N D^k(t)$. Upon a bank's default, consistent with [15], we prioritize meeting deposit withdrawals over repaying inter-bank loans. Connecting the asset and

liability dynamics, we can calculate bank k 's repayment of inter-bank loans owed to bank h , $x_{hk}(t)$ as:

$$x_{hk}(t) = g(y_{hk}(t)) = \begin{cases} y_{hk}(t), & \text{if } A^k(t) \geq V^k(t) + Y^k(t) \\ \max\{0, \frac{y_{hk}(t)}{Y^k(t)}(A^k(t) - V^k(t))\}, & \text{otherwise} \end{cases} \quad (7)$$

That is, after a bank's default, it repays its inter-bank loans to other banks in the network proportionally with any remaining funds upon the satisfaction of deposit withdrawals. Here a bank's incomplete payment to its creditor banks in the network results in financial losses of the creditor banks, therefore facilitating the default risk contagion through counterparty risk. Note that the dependency of $x_{hk}(t)$ on $A^k(t)$ and $V^k(t)$ introduces an inter-bank system feedback, and a link between the financial risk contagion in inter-bank layer (1) and the inter-depositor layer (3).

In the event of a bank default, the bank initiates a fire sale of its assets, resulting in an instant drop in overall investment prices. As per [15], the immediate decrease in market price for investment type m resulting from a fire sale is given by

$$P_m(t) \longrightarrow P_m(t)e^{-\alpha x_m(t)}. \quad (8)$$

Here, $x_m(t)$ is the proportion of security type m held by the bank. This price decline results in financial losses for the banks that have an overlapping investment portfolio, thereby facilitating the spreading of default risk through common asset holdings.

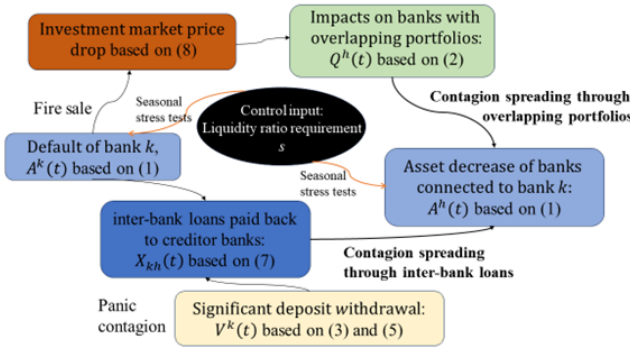


Fig. 1: The Multi-layer default risk contagion process

A flow chart visualizing the multi-layer default risk contagion is shown in Fig. 1. Here, panic contagions over the depositor networks (3) enhance the spreading of the default risk contagion over the inter-bank network through both channels. First, a more aggressive panic contagion could escalate the volume of deposit withdrawals, thereby heightening the risk of inter-bank loan repayment shortfall (7), leading to potential loss of assets for the creditor banks. Second, increased deposit withdrawals elevate banks' liabilities, consequently raising the likelihood of potential bank defaults and subsequent fire sales. This in turn leads to a decrease in the overall market price of investments and financial losses for banks holding common assets with the defaulted bank. A control input, the liquidity ratio input, is included in this

figure to influence the dynamics of banks assets and liability, and thereby the dynamics of bank defaults, which will be further explained in Section IV.

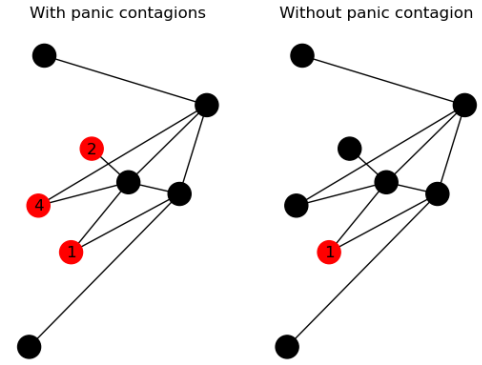


Fig. 2: Default risk spread with vs. without panic contagions

A simulation showing the comparison of the default risk spreading processes with v.s. without panic contagion is shown in Fig. 2; this showcases the propagation of default risk across the inter-bank network subsequent to a financial shock hitting one of the banks, portraying bank defaults that occur ten time steps after the initial shock. Banks highlighted in red indicate those that have defaulted, with explicit labeling of the time step at which each default occurred. It is visually evident that default risk spreads rapidly when panic contagions within each bank are at play, whereas without panic involvement, the default risk remains localized to the initial "patient zero" bank.

III. THE DATA-INFORMED CONTAGION MODEL

The three-year COVID-19 pandemic significantly impacted public health and strained the U.S. economy. In March and April 2023, three major regional banks—SVB, Signature Bank, and First Republic Bank—collapsed [25]. Our model considers the long-term dynamics of financial default risk contagion in the inter-banking system, incorporating key macroeconomic factors such as fluctuating federal interest rates, rising inflation, increased delinquency rates in commercial real estate, and stress on the technology sector. These factors are essential for understanding post-pandemic economic pressures, which we aim to capture through a data-driven model utilizing actual post-pandemic data.

A. System ID with ARMA models

As discussed in Section II-A, a critical element of a bank's asset composition includes investments in both liquid assets (e.g. securities, cryptocurrencies) and non-liquid (e.g. long-term bonds, commercial real estate) assets. Specifically, we assume investments in 5-year and 10-year U.S. Treasury bonds, stocks in technology, pharmaceutical/biotech, commerce companies, and cryptocurrencies. The prices of these investments fluctuate based on market conditions, influenced by the federal interest rate.

To effectively handle temporal dependencies and capture stationary behavior ([26]), we use an $ARMA(p, q)$ model

to estimate and detect trends in post-pandemic investment prices. Specifically, we consider

$$z(t) = a_1 z(t-1) + \dots + a_p z(t-p) + b_1 \tau(t-1) + \dots + b_q \tau(t-q) + e, \quad (9)$$

where z represents the unit market price of investments, τ is the federal interest rate, and e is a white noise disturbance. We estimate the model parameters $a_1, \dots, a_p, b_1, \dots, b_q$ using simple least-square methods (from Python package GEKKO), and determine the model dimensions p, q as the lowest values that yield the highest improvement in terms of estimation error.

The fluctuation in the prices directly affect the total assets of each bank as per (1) and (8). We use the pricing dynamics parameterized in (9) to drive the evolution of the economic incentives and pressure for banks to hold/offload certain assets, highlighting the spread of default risk through common assets holdings, as discussed in II-C.

We collected monthly time series data for U.S. Treasury bond yields, securities, and cryptocurrency prices from January 2020 to August 2023. Sector stock prices were computed as weighted averages of historical prices of key companies: technology (Google, Tesla, Meta, Microsoft), pharmaceuticals (Pfizer, J&J, AbbVie, Moderna), commerce (Amazon, eBay, Walmart, Costco), and cryptocurrencies (Bitcoin, Ethereum). Estimations of investment prices using the ARMA models are shown in Figures 3, 4, 5, respectively.

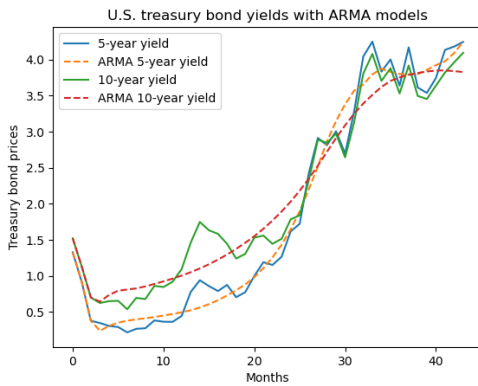


Fig. 3: Identified U.S. treasury bonds yields with ARMA models; $p_{5year} = 3, q_{5year} = 2; p_{10year} = 3, q_{10year} = 2$.

B. Synthetic model parameters

Accessing specific private data, such as individual banks' investment portfolios and depositors' social contact networks, poses challenges in model calibration. To address this, we synthetically generate investment portfolios based on the Fidelity benchmark [27]. Larger core banks are assumed to have "balanced" portfolios with more bonds and cash reserves, while smaller peripheral banks maintain "aggressive" portfolios, emphasizing securities, cryptocurrencies, and commercial real estate loans, reflecting scenarios like the Signature Bank crisis.

We also simulate synthetic social contact networks, assuming that depositors of smaller banks have densely connected

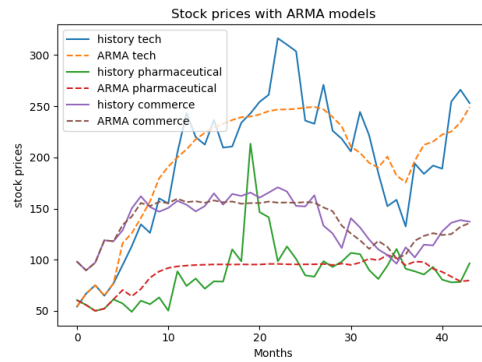


Fig. 4: Identified history stock prices with ARMA models; $p_{tech} = 5, q_{tech} = 4; p_{pharm} = 1, q_{pharm} = 5; p_{commerce} = 5, q_{commerce} = 2$.

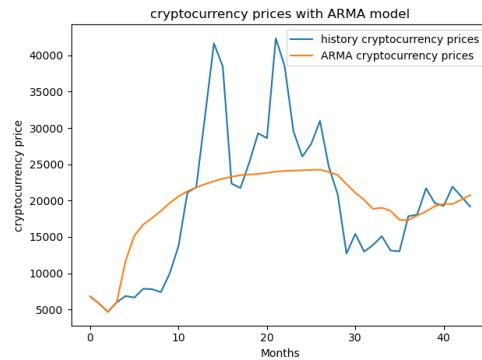


Fig. 5: Identified history cryptocurrency prices with ARMA models; $p_{crypto} = 4, q_{crypto} = 2$.

networks, similar to Silicon Valley Bank, whereas those of larger banks are more sparsely connected. These synthetic parameters allow us to assess how depositor network interconnectedness affects the propagation of default risk in the inter-banking network. Denser depositor networks lead to faster contagion and more bank defaults, as detailed in our simulation results in Section IV-B.

IV. THE OPTIMAL CONTROL PROBLEM

The liquidity stress test is a widely recognized method for assessing a bank's preparedness for potential crises, including bank runs [28], [29]. With the implementation of a uniform liquidity ratio requirement across all banks, important questions arise: What is the relationship between the liquidity ratio and the balance between intra-bank assets and inter-bank loans? What level of liquidity requirement, s , would most effectively mitigate the spread of default risk? In this section, we address the mitigation of default risk contagion as an optimal control problem, using the state dynamics defined in Section II and the uniform liquidity ratio requirement as the control input.

A. Control input: liquidity ratio requirement

We consider a finite time horizon T . To capture the mitigation of default risk, we define the objective function of the optimal control problem as the total number of bank

defaults over T following an initial shock:

$$\min_{s \in [0,1]} J(s) = \sum_{t=1}^T D_t(s), \quad (10)$$

where $D_t(s)$, as previously defined in Section II-C following (6), is the number of bank defaults at time t corresponding to the liquidity ratio requirement s . Asset states $A^k(t)$ are adjusted to $A^k(s,t)$ to meet the liquidity requirement s through asset reallocation as per (1). Each fiscal quarter, a liquidity stress test evaluates the liquidity ratio $Liq^k(t)$ - the proportion of liquid assets to total assets - against s . Banks with $Liq^k(t) < s$ first seek inter-bank loans from the largest core bank. If these loans are insufficient, they resort to fire sales of treasury bonds $Q^k(t)$ and commercial real estate $O^k(t)$, at discounts of 20%, 25%, and 30%, respectively. Significant asset devaluation may trigger depositor panic, modeled by (3).

A low liquidity threshold might not prevent bank runs, exacerbating default risk through asset fire sales and impacting other banks with similar holdings, as described by (8) and (2). Conversely, a high liquidity requirement forces banks to hold more low-yield assets, which may reduce profitability and limit their ability to cope with economic challenges like those seen during the pandemic.

B. Long-term financial contagion simulation

We focus on drawing insights on the optimal policy via simulations. Using the data-informed model from Section III, we simulate a 42-month (13 fiscal quarters) financial contagion scenario to examine the effects of seasonal liquidity requirements on the default risk propagation. The simulation reflects post-pandemic macroeconomic conditions, including rising interest rates, inflation, technology and cryptocurrency market surges, and declining office occupancy impacting commercial real estate.

We model an 8-bank network: 3 large banks (banks 1-3) with balanced portfolios and sparsely connected depositor networks, and 5 small to medium-sized regional banks (banks 4-8) with aggressive portfolios and denser depositor networks. Large banks start with approximately 10,000(k) in assets, diversified across cash, bonds, securities, and cryptocurrencies, while regional banks hold 3000 – 5000(k) with higher allocations in commercial real estate and riskier assets.

Each fiscal quarter begins with a stress test adjusting assets to meet the liquidity requirement s . Inter-bank loans resulting from liquidity adjustments are due at the start of the next quarter. Investment prices update monthly using ARMA models identified in Section III. A panic contagion is triggered if a bank's assets devalue by more than 15% within a quarter, prompting large-scale cash withdrawals. If cash is insufficient, liquid assets are sold first, followed by fire sales of non-liquid assets at discounted prices if necessary, as dictated by equations (5), (8), and (7). Simulations were conducted with liquidity requirements ranging from 0 to 0.9 and varying parameters for panic contagion and depositor network density. We assessed contagion severity by tracking

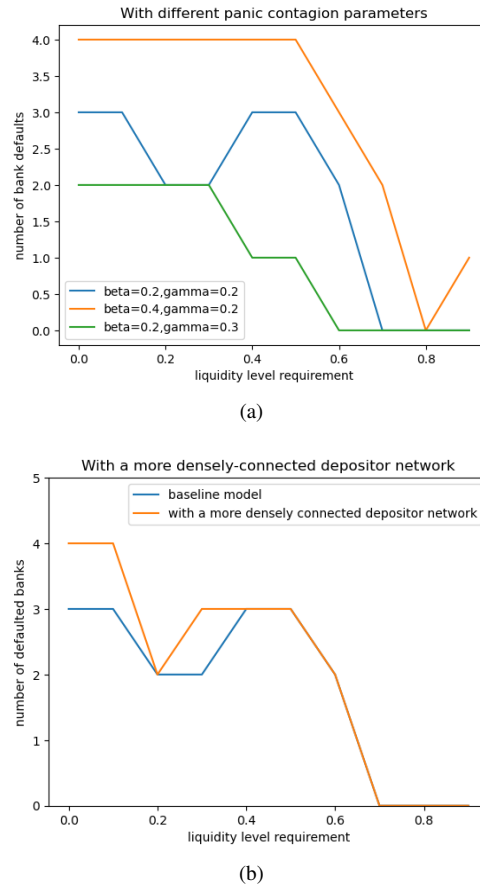


Fig. 6: Long-term bank default simulations with varying liquidity ratio requirements comparing the baseline model to models with different panic contagion parameters: (a) increased panic transmission rate (β), doubling the speed of panic spread (orange); or increased panic recovery rate (γ), with resolution 1.5 times faster than baseline (red); (b) densely connected depositor network (W), with 1000 interconnected depositors for larger banks and 400 for small/medium-sized banks, increasing overall panic spread.

the number of defaults over 42 months and identifying when the first default occurred. Results are shown in Figs. 6a, 6b.

Examining the effects of panic contagion reveals that a more severe panic contagion—due to a higher panic transmission rate β or a denser social network W —leads to increased bank defaults. Conversely, a milder panic contagion, potentially caused by a higher recovery rate γ , results in fewer defaults.

Interestingly, the relationship between the required liquidity level and bank defaults exhibits a threshold pattern. As the liquidity ratio requirement initially increases, the number of bank defaults decreases or remains constant because higher liquidity serves as a buffer against bank runs. However, continued increases in the liquidity ratio can stress the default risk, potentially increasing or maintaining the number of defaults. This can be due to fire sales by banks to meet liquidity requirements, which devalue assets and may trigger more bank runs. In the post-pandemic market, very high liquidity requirements lead to fewer bank defaults, indicating protection against systemic risk. However, this protection

comes at the cost of reduced bank profitability, as banks must hold a larger portion of their assets in liquid form rather than in higher-yielding non-liquid assets.

We also derive the analytical form of the optimal policy for the simple case of a flat market. In this case, the public value for all assets and investments is time-invariant, the optimal liquidity requirement $s^* = c, \forall c \in [0, s^\dagger]$, where s^\dagger satisfies

$$\sum_n (C^n(0) - s^\dagger A^n(0)) = \sum_m (s^\dagger A^m(0) - liq^m(0)), \quad (11)$$

where n, m , respectively denote all the larger-sized and small-to-medium sized regional banks, and $liq^m(0) = C^m(0) + Q_{liq}^m(0)$ is the size of initial liquid assets of bank m . This equation ensures that larger banks have enough extra cash to cover any liquidity shortfall in regional banks, allowing for liquidity adjustments through inter-bank loans without causing fire sales. Rigorous analysis and derivation of optimal policies for more complex cases is deferred to future work.

V. CONCLUSION

We've proposed a multi-layer default risk contagion model for inter-banking networks, introducing a novel layer of panic contagion that explicitly captures the dynamics and influence of intra-bank runs. Our model is calibrated to post-COVID financial data, providing a comprehensive understanding of long-term default risk dynamics while accounting for market fluctuations and macroeconomic factors. System identification techniques allow for model calibration and formulation of an optimal control problem related to liquidity ratio requirements during seasonal banking stress tests. Simulations with varying control inputs reveal intriguing threshold structures in the optimal policy, suggesting further avenues for exploration. The detailed characterization and refinement of these optimal stress testing policies will be addressed in future work.

DISCLAIMER

This paper was prepared for informational purposes in part by the Artificial Intelligence Research group of JPMorgan Chase & Co. and its affiliates ("JP Morgan"), and is not a product of the Research Department of JP Morgan. JP Morgan makes no representation and warranty whatsoever and disclaims all liability for the completeness, accuracy or reliability of the information herein. This document is not intended as investment research or investment advice, or a recommendation, offer or solicitation for the purchase or sale of any security, financial instrument, financial product or service, or to be used in any way for evaluating the merits of participating in any transaction, and shall not constitute a solicitation under any jurisdiction or to any person, if such solicitation under such jurisdiction or to such person would be unlawful.

REFERENCES

- [1] D. Acemoglu, A. Ozdaglar, and A. Tahbaz-Salehi, "Systemic risk and stability in financial networks," *American Economic Review*, vol. 105, no. 2, pp. 564–608, 2015.
- [2] M. Boss, H. Elsinger, M. Summer, and S. Thurner, "Network topology of the interbank market," *Quantitative finance*, vol. 4, no. 6, pp. 677–684, 2004.
- [3] G. Brandi, R. Di Clemente, and G. Cimini, "Epidemics of liquidity shortages in interbank markets," *Physica A: Statistical Mechanics and its Applications*, vol. 507, pp. 255–267, 2018.

- [4] P. Jorion and G. Zhang, "Credit contagion from counterparty risk," *The Journal of Finance*, vol. 64, no. 5, pp. 2053–2087, 2009.
- [5] F. Caccioli, J. D. Farmer, N. Foti, and D. Rockmore, "Overlapping portfolios, contagion, and financial stability," *Journal of Economic Dynamics and Control*, vol. 51, pp. 50–63, 2015.
- [6] M. Montagna and C. Kok, "Multi-layered interbank model for assessing systemic risk," 2016.
- [7] S. Poledna, J. L. Molina-Borboa, S. Martínez-Jaramillo, M. Van Der Leij, and S. Thurner, "The multi-layer network nature of systemic risk and its implications for the costs of financial crises," *Journal of Financial Stability*, vol. 20, pp. 70–81, 2015.
- [8] T. Lux, "A model of the topology of the bank–firm credit network and its role as channel of contagion," *Journal of Economic Dynamics and Control*, vol. 66, pp. 36–53, 2016.
- [9] S. Jiang, J. Wang, R. Dong, Y. Li, and M. Xia, "Systemic risk with multi-channel risk contagion in the interbank market," *Sustainability*, vol. 15, no. 3, p. 2727, 2023.
- [10] S. Jiang and H. Fan, "Credit risk contagion coupling with sentiment contagion," *Physica A: Statistical Mechanics and Its Applications*, vol. 512, pp. 186–202, 2018.
- [11] Q. Qian, H. Feng, and J. Gu, "The influence of risk attitude on credit risk contagion—perspective of information dissemination," *Physica A: Statistical Mechanics and its Applications*, vol. 582, p. 126226, 2021.
- [12] T. Chen, Y. Wang, Q. Zeng, and J. Luo, "Network model of credit risk contagion in the interbank market by considering bank runs and the fire sale of external assets," *Physica A: Statistical Mechanics and Its Applications*, vol. 542, p. 123006, 2020.
- [13] X.-L. Gong, J.-M. Liu, X. Xiong, and W. Zhang, "Research on stock volatility risk and investor sentiment contagion from the perspective of multi-layer dynamic network," *International Review of Financial Analysis*, vol. 84, p. 102359, 2022.
- [14] The American Deposit Management Co., "A brief history of u.s. bank failures," 2023, [Online; accessed 6-March-2024]. [Online]. Available: <https://americandeposits.com/brief-history-us-bank-failures/>
- [15] P. Shen and Z. Li, "Financial contagion in inter-bank networks with overlapping portfolios," *Journal of Economic Interaction and Coordination*, vol. 15, pp. 845–865, 2019.
- [16] C.-P. Georg, "The effect of the interbank network structure on contagion and common shocks," *Journal of Banking & Finance*, vol. 37, no. 7, pp. 2216–2228, 2013.
- [17] G. G. Kaufman, "Bank runs: causes, benefits, and costs," *Cato J.*, vol. 7, p. 559, 1987.
- [18] M. Brown, S. T. Trautmann, and R. Vlahu, "Understanding bank-run contagion," *Management Science*, vol. 63, no. 7, pp. 2272–2282, 2017.
- [19] D. P. Maki, "Mathematical models and applications: with emphasis on the social, life, and management sciences," 1973.
- [20] J. M. Epstein, J. Parker, D. Cummings, and R. A. Hammond, "Coupled contagion dynamics of fear and disease: mathematical and computational explorations," *PloS one*, vol. 3, no. 12, p. e3955, 2008.
- [21] L. Zhao, H. Cui, X. Qiu, X. Wang, and J. Wang, "SIR rumor spreading model in the new media age," *Physica A: Statistical Mechanics and its Applications*, vol. 392, no. 4, pp. 995–1003, 2013.
- [22] L. Fu, W. Song, W. Lv, and S. Lo, "Simulation of emotional contagion using modified SIR model: A cellular automaton approach," *Physica A: Statistical Mechanics and its Applications*, vol. 405, pp. 380–391, 2014.
- [23] N. A. Ruhi, H. J. Ahn, and B. Hassibi, "Analysis of exact and approximated epidemic models over complex networks," *arXiv preprint arXiv:1609.09565*, 2016.
- [24] "Default (finance) - Wikipedia, the free encyclopedia," 2024, [Online; accessed 6-March-2024]. [Online]. Available: [https://en.wikipedia.org/wiki/Default_\(finance\)](https://en.wikipedia.org/wiki/Default_(finance))
- [25] L. Rodini, "Looking back at the banking crisis of 2023," *TheStreet*. [Online]. Available: <https://www.thestreet.com/personal-finance/american-finance/>
- [26] R. S. Tsay, *Analysis of financial time series*. John Wiley & sons, 2005.
- [27] "Fidelity fund portfolios—diversified," 2024, [Online; accessed 6-March-2024]. [Online]. Available: <https://www.fidelity.com/mutual-funds/fidelity-fund-portfolios/overview>
- [28] T. Schuermann, "Stress testing banks," *International Journal of Forecasting*, vol. 30, no. 3, pp. 717–728, 2014.
- [29] P. Grundke and A. Kühn, "The impact of the basel iii liquidity ratios on banks: Evidence from a simulation study," *The Quarterly Review of Economics and Finance*, vol. 75, pp. 167–190, 2020.